Chapter 5

# OPTICAL COMB DYNAMICS AND STABILIZATION

Günter Steinmeyer[1] and Ursula Keller[2]
[1]*Max-Born-Institut für Nichtlineare Optik und Kurzzeitspektroskopie*

[2]*Institut für Quantenelektronik, ETH Zürich*

**Abstract:** The spectrum of a mode-locked laser consists of a comb of equidistantly spaced frequencies. This comb has only two degrees of freedom, its offset frequency at zero and the spacing of the teeth of the comb. While the spacing of the frequencies is simply determined by the repetition rate of the laser and can be relatively easily controlled, the offset frequency is governed by phase differences between the carrier and the envelope of the pulses during one round trip through the laser cavity. This carrier-envelope offset (CEO) phase is measured via heterodyning different harmonics of the mode-locked laser spectrum. In an unstabilized laser, this CEO phase exhibits very strong noise and can fluctuate several thousand radians in only one second. We provide an analysis of CEO phase-noise contributions and track their origin. The passive stability with respect to CEO fluctuations can be greatly improved by suitable cavity design, which greatly simplifies the stabilization of the CEO phase. Recent efforts on carrier-envelope stabilization are reviewed and some limitations are outlined.

**Key words:** dispersion, carrier-envelope phase, phase noise, phase stabilization

## 1. INTRODUCTION

Ultrashort pulse generation reached pulse durations of a few femtoseconds around the turn of the century [1]. Some of the shortest pulses have a width of only two optical cycles [2-4]. When pulse durations approach this regime, the commonly used approach of the slowly varying envelope approximation (SVEA) starts to fail. Nonlinear optical effects are then expected to depend not only on the envelope structure of the pulses, but also on the structure of the electric field itself, including its relative phase to



the envelope, which has been referred to as the absolute phase. In 2001 and 2003, the first experimental evidence for the failure of the SVEA was reported [5].

In this chapter, we describe how to monitor the relative phase between the envelope and the carrier of an optical pulse train from a mode-locked optical oscillator. The chapter is organized as follows: First, we introduce the definition of the carrier-envelope-offset (CEO) phase and frequency. We show how both entities are connected with intracavity dispersion. Methods to measure the CEO frequency are discussed, with an emphasis on the most wide spread $\nu$-to-$2\nu$ scheme. Careful characterizations of the CEO-phase-noise spectra are used to isolate the physical mechanisms behind the excessive fluctuations of the CEO phase of a free-running oscillator. This insight allows building femtosecond lasers with an increased passive stability of the CEO and forms the basis for subsequent stabilization of the CEO frequency. Finally, we discuss how to optimize control of the CEO phase and how to push residual phase jitter into the attosecond range.

## 2. COMB PARAMETERS AND THEIR CONNECTION TO INTRACAVITY DISPERSION

### 2.1 Carrier-envelope-offset phase and frequency in the time domain

Figure 5-1 shows the envelope and the carrier of two subsequent pulses from a mode-locked laser. The envelope travels at group velocity $\upsilon_g = c/n_g = c/(n+\omega\, dn/d\omega)$ and repeats itself after the cavity round-trip time $T_R$. The underlying carrier propagates at phase velocity $\upsilon_p = c/n$. Generally, $\upsilon_p \neq \upsilon_g$ in any dispersive medium. This means that the electric-field structure of the pulse will undergo a permanent change. The drift of the relative phase between carrier and envelope can be tracked down to the $dn/d\omega$ term in the definition of the group velocity.

When propagating through a dispersive material with an index of refraction $n(z)$ along the axis $z$, the pulse will accumulate a phase offset between the carrier and envelope of

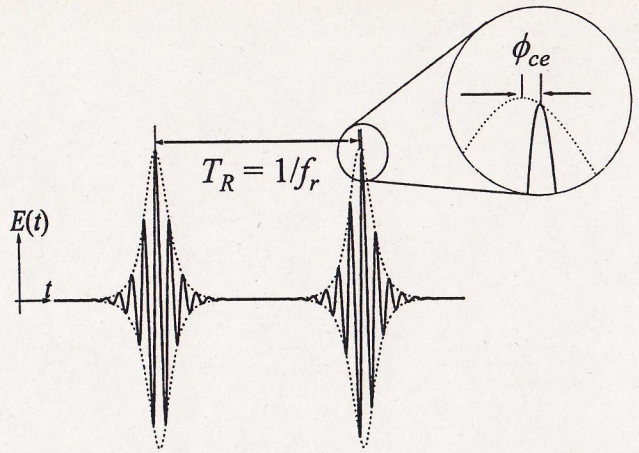


*Figure 5-1.* The electric field $E(t)$ of two subsequent pulses from a mode-locked laser (solid line). The envelope $\pm A(t)$ is shown as dashed lines. The electric-field patterns of the pulses experience a pulse-to-pulse phase shift $\Delta\phi_{ce}$ according to Equation (1).

$$\Delta\phi_{ce} = \left[\frac{2\pi}{\lambda}\int_0^L n_g(z) - n(z)\,\mathrm{d}z\right] \bmod 2\pi = \left[\frac{\omega^2}{c}\int_0^L \frac{dn(z)}{\mathrm{d}\omega}\,\mathrm{d}z\right] \bmod 2\pi. \quad (1)$$

Here $L$ is the length of the dispersive material. For the case of a linear cavity, $L$ takes the role of twice the cavity length, and the carrier-envelope offset (CEO) phase $\Delta\phi_{ce}$ is the change of the phase $\phi_{ce}$ per round trip:

$$\Delta\phi_{ce}(t) = \phi_{ce}(t) - \phi_{ce}(t - T_R)\,. \quad (2)$$

The CEO phase $\Delta\phi_{ce}$ must not be confused with the phase $\phi_{ce}$, which is typically defined such that a pulse with $\phi_{ce} = 0$ has the largest possible value of the electric field [6]. Some authors have referred to $\phi_{ce}$ as the absolute phase. An example for such a pulse is shown as the left pulse in Figure 5-1. $\Delta\phi_{ce}$, however, is defined as the difference of the absolute phase of two subsequent pulses. It is useful to introduce the CEO frequency [7]

$$f_0 = \frac{\Delta\phi_{ce}}{2\pi} f_r\,, \quad (3)$$

where $f_r$ equals the inverse round-trip time $1/T_R$ of the cavity and $f_0$ is time dependent unless the intracavity dispersion and the cavity length are



absolutely constant with time. Changes of $f_0$ or $\Delta\phi_{ce}$ tend to be unnoticeably small on a pulse-to-pulse time scale but can reach significant magnitudes on millisecond time scales, rendering stabilization of these parameters a nontrivial task. For a detailed derivation of the fundamental comb parameters from periodic waveforms and their connection to intracavity dispersion, we refer the reader to Reference [8].

## 2.2 The frequency comb and its dynamics

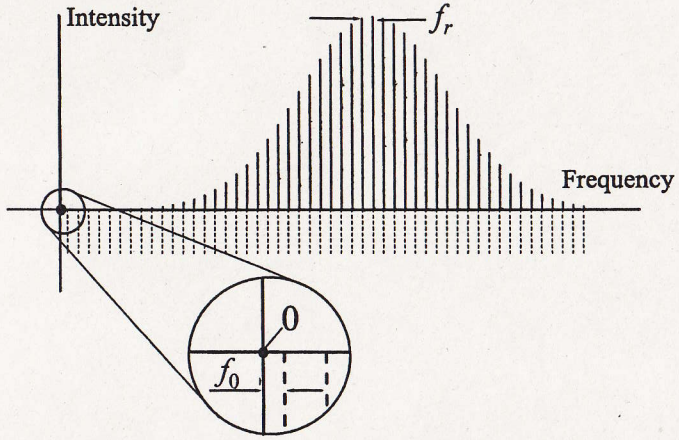


*Figure 5-2.* Equidistant frequency comb of a mode-locked laser. The comb lines are spaced by the repetition rate $f_r$ and exhibit a nonvanishing offset frequency $f_0$ at zero frequency unless the electric-field pattern exactly reproduces from pulse to pulse (compare to the time domain picture in Figure 5-1).

For the following considerations, it is useful to revisit the scenario of Figure 5-1 in the Fourier domain. As the pulses follow each other at a constant delay $T_R$, their spectrum consists of a comb of equidistantly spaced frequencies with a separation $f_r = 1/T_R$. This frequency comb must not be confused with the modes of a linear cavity, which are only equidistant in the absence of intracavity dispersion. In contrast, if the spacing between the teeth in the mode-locked frequency comb were not constant, different Fourier components of the pulse in Figure 5-1 would travel at different repetition rates inside the cavity, and the pulse would slowly, but surely, drift apart. The fact that the separation of the frequencies is constant over the entire comb has been experimentally checked to better than $10^{-15}$ [9].

Differing phase and group velocity cause a translation of the entire frequency comb by the carrier-envelope-offset frequency $f_0$. The frequencies of the $i^{\text{th}}$ comb component can therefore be written in the form:

$$\nu_i = f_0 + i f_r . \tag{4}$$

This leaves only two degrees of freedom for the dynamics of the frequency comb, translation via $f_0$ and breathing via $f_r$, as illustrated in Figure 5-3. Any kind of perturbation of the cavity, e.g., by a thermal change of the refractive index of the laser crystal, will typically affect both the repetition rate and the CEO frequency.

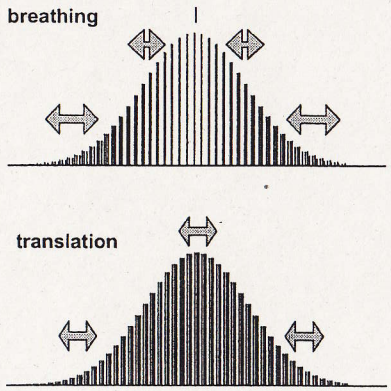


*Figure 5-3.* Comb dynamics [10]. The frequencies inside the comb structure are determined by two parameters, $f_0$ and $f_r$. This gives rise to a translational degree of freedom and a breathing mode. Noise contributions will induce a characteristic linear combination of both degrees of freedom.

However, there is always a fixed frequency $f_x$ that remains unaffected by a distortion $X$ [11].

$$f_x = f_0 + f_r \frac{\partial f_0}{\partial X}\left(\frac{\partial f_r}{\partial X}\right)^{-1}, \tag{5}$$

where $X$ could be any physical parameter of the cavity, e.g., its length or the temperature of the laser crystal. Let us illustrate the concept of a fixed point by choosing $X$ as the cavity length. Cavity length fluctuations only affect the repetition rate $f_r$ of the laser but leave the per-round-trip phase shift $\Delta\phi_{ce}$ between envelope and carrier unchanged. Inserting Equation (3) into Equation (5) yields $f_x = 2f_0$, i.e., a value very close to zero frequency. A complementary example would be an effect that causes only a change of the cavity group delay but leaves the phase delay unchanged. This could be achieved, e.g., by tilting a mirror in an intracavity prism sequence with the pivot point adjusted to the center frequency of the mode-locked spectrum



[12]. Retarding the group by one cycle relative to the phase changes $f_0$ by one free spectral range (i.e., the repetition rate), whereas the repetition rate itself only changes by a very small amount. In this case, one calculates that $f_x$ equals the carrier frequency of the pulse. Most environmental contributions to comb dynamics, such as thermal or nonlinear changes of the intracavity refractive indices, have an $f_x$ located between zero frequency and the carrier frequency [11]. This means that they neither add a pure contribution to the group delay nor do they only affect the phase delay of the group. Measuring the fixed frequency $f_x$ can help to pinpoint the source of dominant frequency comb dynamics.

## 3. MEASUREMENT OF THE CEO FREQUENCY

An early approach for measurement of $f_0$ employed an interferometric method based on second-harmonic generation (SHG) cross-correlation between two subsequent laser pulses [13]. For vanishing $\Delta\phi_{ce}$, the cross-correlation signal is identical to the interferometric autocorrelation, with a symmetric fringe pattern. In all other cases, the fringe pattern appears shifted with the fringe maximum located at $\Delta\phi_{ce}/\omega_c$ and the cross-correlation is asymmetric. Even though this measurement in the time domain works in principle [14], it is very susceptible to offset errors. Any offset between group and phase delay in the long arm of the cross-correlator will induce a measurement error in determining $f_0$. Therefore, phase-coherent methods are indispensable for precise control of the CEO phase as was suggested in Reference [6].

### 3.1 Heterodyning different laser harmonics

Figure 5-4 provides the key to the measurement of $f_0$ by heterodyning harmonics from different parts of the mode-locked spectrum. The technique was first proposed by Telle et al. [6]. Taking the $N^{\text{th}}$ harmonic of a comb line $N\nu_{m_1} = Nf_0 + Nm_1 f_r$ and beating it with the $M^{\text{th}}$ harmonic of another comb line $M\nu_{m_2} = Mf_0 + Mm_2 f_r$ yields

$$N\nu_{m_1} - M\nu_{m_2} = (N-M)f_0, \tag{6}$$

which requires that $Nm_1 = Mm_2$. Equation (6) is the key to any measurement of the carrier-envelope offset and was used in the first experimental demonstrations by Jones et al. [14] and Apolonski et al. [15] for the case of

$N = 1$. The beat note of Equation (6) delivers the carrier-envelope-phase-slippage rate, either directly or as one of its harmonics. An example for a measurement of the CEO frequency, which is based on this scheme, is shown in Figure 5-5.

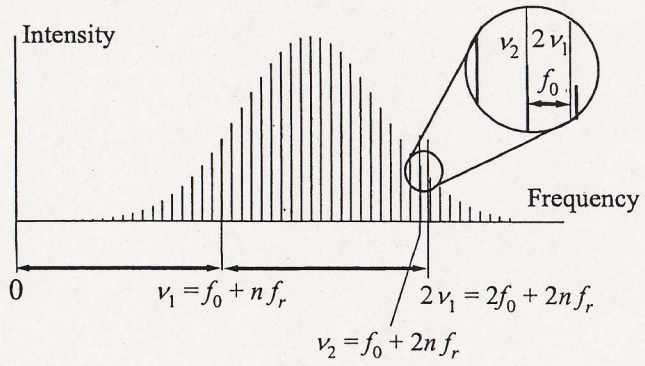


***Figure 5-4.*** Scheme for measuring the CEO-frequency of a laser comb for the case of heterodyning the fundamental and the second harmonic, i.e., $N = 1$ and $M = 2$ in Equation (6). Graphically, this scheme mirrors the origin at $f = \nu_1$, transferring the $f_0$ beat from dc into a region with nonvanishing spectral content.

However, the scheme of Equation (6) requires a certain minimum spectral width of the comb $\Delta\nu/\nu = 2(N-M)/(N+M)$; e.g., beating of the fundamental and second harmonic requires an optical octave of bandwidth with $\Delta\nu/\nu = 0.67$. The situation of second-harmonic generation is illustrated in Figure 5-4. Often, an octave-spanning spectrum is not directly available from the oscillator. Alternatively, one can meet the bandwidth requirement by additional external broadening, as shown in the schematic setup in Figure 5-6, which is actually the most commonly used scheme to measure the CEO frequency of a laser.



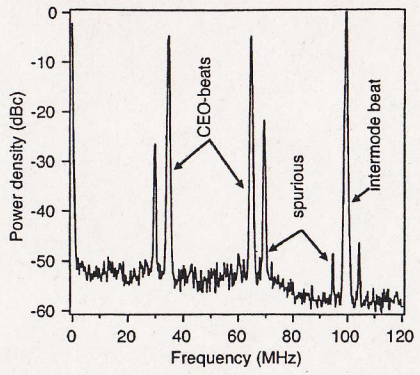


*Figure 5-5.* Typical rf spectrum of the CEO beat note signal. This signal was measured at a Ti:sapphire laser heterodyning the fundamental and the second-harmonic-generation (SHG) signal from a continuum generated in a microstructure fiber [16]. The CEO beat is located at 35 MHz with a signal-to-noise ratio of >45 dB in a 100 kHz bandwidth. Its mirror frequency is also visible at 65 MHz. The laser has a 100 MHz repetition rate. Some spurious contributions have been generated by nonlinear electronic mixing processes in the detector circuitry.

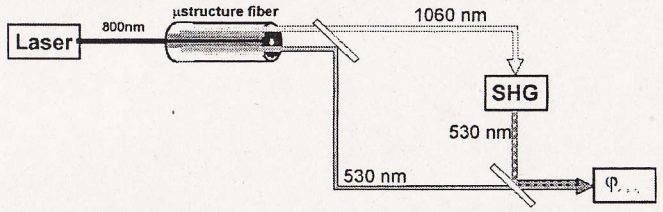


*Figure 5-6.* Schematic drawing of a practical implementation of Equation (6) and Figure 5-4. The laser is spectrally broadened to more than an optical octave using continuum generation in a microstructure fiber. Two wavelengths forming one octave are separated. The long-wavelength component is frequency doubled and heterodyned with the fundamental signal. The beat note contains an rf component at the CEO frequency. Specific wavelengths shown are meant as example values.

## 3.2 Transfer oscillators and interval bisection

Let us briefly mention other ways to circumvent the bandwidth bottleneck [6]. These alternative methods rely on transfer oscillators and interval bisection. A transfer oscillator is an additional single-frequency cw laser with frequency $\nu_{trans}$. This frequency or one of its harmonics has to be locked to one of the comb frequencies. At the same time, the fundamental

transfer oscillator is used for sum-frequency generation from the low-frequency part of the comb to the high-frequency part. The beat notes of both then allow extraction of the CEO frequency. In particular, when the second or third harmonic of the transfer oscillator can be generated at sufficient power, this scheme can be operated with smaller bandwidth requirements. If the second harmonic of the transfer oscillator is locked to the comb, only 0.6 of an optical octave is required in the comb. For third-harmonic generation, only 0.4 optical-octave bandwidth is required.

Frequency-interval bisection [17] can be employed to divide the required comb width. The simplest scheme of this type uses a one-octave interval-divider stage that generates the frequency $\nu_a$ at the midpoint of $\nu_b$ and $2\nu_b$. This can be done by phase locking the second harmonic of $\nu_a$ to the sum frequency of $\nu_b$ and $2\nu_b$ to yield

$$\frac{\nu_a}{2\nu_b} = \frac{3\nu_b/2}{2\nu_b} = \frac{3}{4}. \tag{7}$$

This way, one now has available two phase-locked oscillators at only half-an-octave spectral separation. Locking one to the comb and phase comparison of the other allow extraction of the CEO frequency of the comb.

## 4. CEO PHASE NOISE

From the discussion so far, it should be clear that the carrier-envelope phase of a femtosecond oscillator is extremely sensitive to any kind of environmental influence and changes of the laser parameters such as pulse duration or power fluctuations. In this section, we discuss measurements of the carrier-envelope-phase noise of a laser oscillator. From these measurements, one can judge the severity of the noise problem. It is also helpful to reach an understanding of the mechanisms behind the carrier-envelope-phase noise before attempting to stabilize the CEO phase. For this reason, we discuss measurements of the CEO phase noise for different laser configurations. We restrict ourselves to measurements of Ti:sapphire lasers, as the CEO-phase noise in these lasers has been analyzed with great scrutiny. The general carrier-envelope-phase noise shows striking similarities with timing-jitter noise in mode-locked lasers [18, 19]. We therefore use a similar formalism to describe and analyze the dynamics of the carrier-envelope-offset frequency and phase.



### 4.1 Noise densities and rms phase jitter

The easiest way to characterize the CEO-noise properties consists of frequency-to-voltage conversion of the CEO beat noise and subsequent spectral analysis with a Fourier analyzer or a similar spectrum analyzer. Multiplying the measured voltage noise by the conversion factor of the frequency-to-voltage converter yields the single-sideband frequency noise density $\sigma_{f_0}(f)$ in units $\mathrm{Hz}/\sqrt{\mathrm{Hz}}$ vs Fourier frequency $f$ [16]. Other ways to measure the frequency noise density have been described in [20]. However, the latter approach relied on constant amplitude-to-phase coupling over the entire measurement range. The frequency-noise density can be easily converted into a phase-noise density using the identity

$$\sigma_{\phi_{ce}} = \frac{\sigma_{f_0}}{f}. \tag{8}$$

For an interpretation of the noise data, it is sometimes more useful to integrate the noise densities according to

$$\delta f_0(f_{low}) = \sqrt{2\int_{f_{low}}^{f_r/2} \sigma_{f_0}^2 \, df}, \qquad \delta\phi_{ce}(f_{low}) = \sqrt{2\int_{f_{low}}^{f_r/2} \left(\frac{\sigma_{f_0}}{f}\right)^2 df}. \tag{9}$$

The integration spans from a lower frequency $f_{low}$ given by the inverse measurement time to an upper bound that is ideally half the repetition rate itself. Typically, one can only carry the integration to a few tens or hundreds of kilohertz, which is normally considered sufficient as the noise rolls off very rapidly at high frequencies. The integrated noise densities $\delta\phi_{ce}(f_{low})$ and $\delta f_0(f_{low})$ can be interpreted as rms widths of the fluctuation range of phase or frequency, respectively.

### 4.2 CEO-phase noise of mode-locked oscillators

Examples of phase-noise measurements are shown in Figures 5-7 and 5-8 [16, 21]. From the data in Figure 5-7, one can see that the noise generally rolls off above 1 kHz. At the very end of the measurement range shown in Figure 5-7, there seems to be an increase of noise that may be explainable by relaxation oscillations, similar to observations of timing-jitter noise [19]. The major noise contributions, however, are located in the range of a few 100 Hz to 1 kHz. For an interpretation of the severity of the noise, it is useful to

inspect the integrated phase noise starting at high frequencies and locating the point where the $\delta\phi_{ce}$ approaches unity. In Figure 5-8, one can clearly see that the integrated phase noise already reaches one radian at several kHz Fourier frequency. Around 1 kHz, the noise grows dramatically, reaching values of several hundred to thousands of radians at 100 Hz offset frequency. In summary, this means that severe phase-noise contributions accumulate within approximately 1 ms of measurement time. For a successful phase lock of the CEO frequency, however, it is mandatory to keep residual jitters below $\delta\phi_{ce} \approx 0.3$ rad [22]. This requirement is only set by the cycle-slip-free functioning of the phase-locked loop, whereas applications may demand an even tighter locking to smaller jitter values. These considerations make it clear that for any meaningful stabilization of the CEO frequency, servo bandwidths of 10 kHz or more are required, which makes the use of acousto-optic or electro-optic controls preferable to a mechanical adjustment of intracavity dispersion.

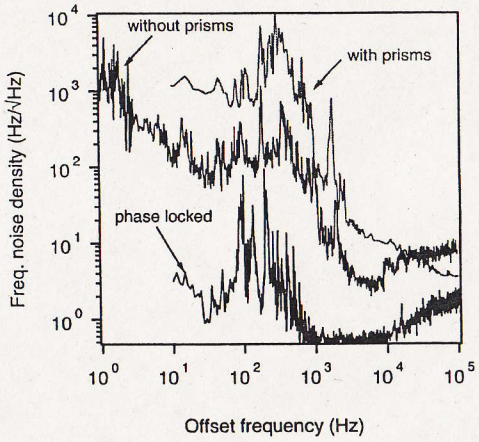


*Figure 5-7.* Frequency noise density of different Ti:sapphire lasers [16, 21]. The top trace shows a measurement for a laser with intracavity prisms; the middle trace is measured for a prismless variant of the same laser. The bottom trace shows how the measured frequency noise density drops farther when a phase lock to a reference oscillator is activated. This measurement has to be interpreted as a noise floor, as it is limited by the stability of the local oscillator in the measurement.

Moreover, Figures 5-7 and 5-8 contain measurements for both oscillators with and without prisms for intracavity dispersion compensation. In these measurements, an identical pump laser was used for the prismless and the prism setup. It becomes evident that prism-based femtosecond oscillators are about ten times as noisy as prismless lasers. This can only be explained by an additional physical mechanism present because of the intracavity prisms.



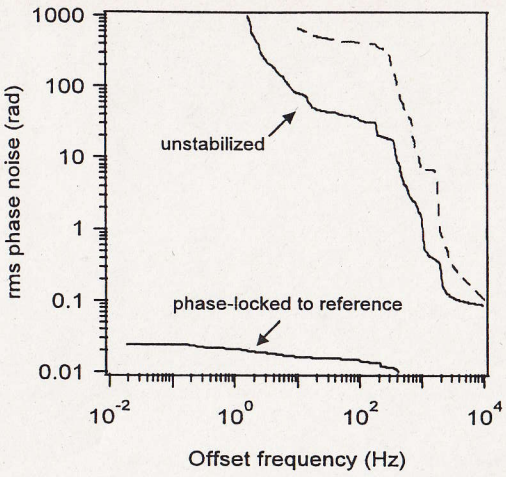


*Figure 5-8.* Integrated phase-noise density of different Ti:sapphire lasers [16, 21]. The top and middle traces have been computed from the data displayed in Figure 5-7 using Equations (8) and (9). The bottom trace is based on a direct phase comparison of a stabilized oscillator and an rf reference using an rf lock-in amplifier.

## 4.3 Physical mechanisms behind CEO fluctuations

The key to understanding the mechanisms forming the CEO noise is Equation (1). Any change of temperature, air pressure, or laser power may also affect $\Delta\phi_{ce}$. For simplicity, let us assume that we have a laser cavity of length $L$ filled with a material of index $n$. We can then rewrite the dependence of Equation (1) on any laser or environmental parameter $X$ as [13, 21, 23]:

$$\frac{\partial}{\partial X}\Delta\phi_{ce} = 2\omega_c \frac{\partial\omega_c}{\partial X}\frac{\partial n}{\partial \omega}L + \omega_c^2 \frac{\partial n}{\partial \omega}\frac{\partial L}{\partial X} + \omega_c^2 \frac{\partial^2 n}{\partial \omega \partial X}L. \qquad (10)$$

These three partial derivatives account for changes of the center frequency $\omega_c$ [13], changes of the cavity geometry [21], and changes of the first-order dispersion of the cavity [16, 23], respectively. Let us first consider environmental effects, which equal $X$ for temperature or air pressure. Temperature changes of the laser crystal or intracavity prisms immediately translate into changes of the CEO frequency. Nevertheless, such variations are relatively slow and cannot fully explain the noise contributions at the high Fourier frequencies well above 1 kHz in Figures 5-7 and 5-8. A similar argument holds for pressure variations, which couple to the CEO frequency by refraction changes caused by the air in the cavity. Another coupling

mechanism is displacement of the cavity mirrors. The latter effect is much less of a concern than for stabilization of single-frequency lasers, because the fixed frequency of the comb dynamics lies close to zero frequency. Thus there is only a negligible effect on $f_0$. In summary, environmental contributions are an important input to the low-frequency part of the CEO noise spectrum. Nevertheless, they can be relatively easily reduced by enclosing the laser in a box, thereby avoiding air turbulence. Typically, environmental contributions can be suitably reduced by these passive measures. Therefore they rarely represent an obstacle to successful stabilization of the CEO frequency.

## 4.4 Amplitude-to-phase conversion effects

Amplitude-to-phase conversion (APC) is a special case of Equation (10). The case where $X$ is the intensity deserves special attention, as the resulting fluctuations of $\Delta\phi_{ce}$ can be arbitrarily fast when electronic nonlinearities such as the all-optical Kerr effect are mediating between amplitude fluctuations and CEO-phase noise. APC effects are mainly taking place in the laser crystal, as this is the position of highest intracavity intensities.

Spectral shifting of the laser spectrum has been proposed as the first mechanism giving rise to APC effects [13]. The carrier frequency $\omega_c$ shifts with pump power or intracavity intensity, an effect that strongly depends on the operating conditions of the laser. Generally, both effects seem to be weaker when the laser bandwidth is wider. In a recent publication, spectral shifting was observed for a 750 MHz repetition-rate laser below 50 nm mode-locked bandwidth, whereas it did not appear to play a role in a 100 MHz repetition-rate laser with its stronger mode locking and higher pulse energy [23]. APC coefficients $\partial f_0 / \partial I$ on the order of $10^{-7}$ HzW/m$^2$ were observed when spectral shifting dominates the APC, resulting in the prevalent contribution to Equation (9). In contrast, the APC coefficient drops to a few $10^{-9}$ HzW/m$^2$ in the absence of spectral shifting [16, 21, 23].

A second contribution to CEO-phase noise arises from geometrical changes of the laser cavity affecting the total cavity length $L$. This contribution is typically negligible in prismless cavities but can play a role in cavities that use intracavity prism sequences for dispersion compensation [3, 21]. One potential mechanism behind such laser dynamics is beam-pointing variations inside the laser cavity together with the directional sensitivity of the dispersion of a prism compressor [21, 24]. If the beam direction inside the prism sequence changes, this will also affect the net first-order dispersion of the cavity via the second term in Equation (10). Beam-pointing variations can be induced by changes of the refractive index of the laser crystal. If the index of refraction of the laser crystal changes, Snell's law demands a change



of angles inside and outside the laser crystal [21]. Beam-pointing effects are held responsible for an approximately tenfold increase of CEO-phase noise of prism laser cavities as compared to prismless variants.

The third term in Equation (10) contains contributions to CEO-phase noise via intensity-induced changes of the refractive index [25]. Nonlinear refraction is well known as the all-optical Kerr effect [26], but according to Equation (10), only the dispersion of the Kerr effect affects changes of the CEO phase. The issue of dispersion of the Kerr effect has been addressed by [27, 28]. According to Sheik-Bahae et al. [27], the main contribution to the first-order dispersion of a dielectric medium well below half the band edge stems from a Kramers-Kronig term induced by two-photon absorption. As per their example, for sapphire at 800 nm, one calculates $\partial^2 n / \partial\omega\, \partial I \approx 10^{-36}$ s m$^2$/W rad. Inserting values for typical Ti:sapphire laser cavities [4], one computes a theoretical estimate of $\partial f_0 / \partial I = 5\times10^{-9}$ HzW/m$^2$, which agrees well with the lowest experimentally observed values of $\partial f_0 / \partial I$. Again, these low APC coefficients can only be reached in the absence of geometrical effects and spectral shifting.

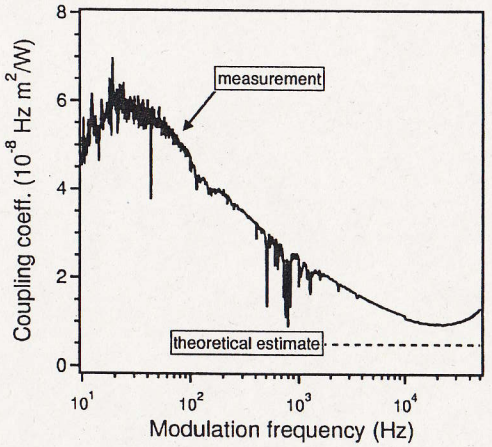


*Figure 5-9.* Transfer function of laser intensity noise into fluctuations of the CEO frequency [16]. These measurements were done in a prismless laser in the absence of spectral shifting. The measurements reflect Kerr contributions to the APC and thermally induced amplitude-to-phase conversion (APC) effects at low frequencies.

A measurement of the APC coefficient is shown in Figure 5-9. The theoretical estimate from Reference [27] is shown as a dashed line. The measurement was performed at different modulation frequencies. For frequencies below 1 kHz, an APC coefficient of a few times $10^{-8}$ HzW/m$^2$ is observed. At higher modulation frequencies, the APC levels off to about $10^{-8}$

HzW/m$^2$. Spectral shifting does not seem to play a role in these experiments, and geometrical effects are also not a concern because of a prismless cavity. At lower frequencies, additional contributions from thermally induced changes of the refractive index increase the APC effect. For modulation frequencies of about 10 kHz or more, the coupling dynamics appear to be restricted to a purely electronic-refractive nonlinearity.

From the experimental observations, some guidelines can be given on how to keep APC effects to a minimum. The first recommendation is to use a prismless cavity, which is also strongly supported by the data in Figures 5-7 and 5-8. In prismless cavities, beam pointing does not translate into CEO-phase noise [21]. Spectral shifting is the other APC effect that can be avoided by suitable design of the laser. For a stable position of the laser spectrum, a broad mode-locked bandwidth of more than 50 nanometers and a high pulse energy appear to be favorable conditions [23]. If geometric effects and spectral shifting can be avoided, the APC effects are restricted to nonlinear refractive mechanisms, both Kerr-type and an additional thermally induced mechanism at low Fourier frequencies. Values on the order of $\partial f_0 / \partial I = 10^{-8}$ HzW/m$^2$ or less are indicative of a dominance of nonlinear refraction in the APC dynamics.

# 5. STABILIZATION OF THE CEO FREQUENCY

In previous sections, we have introduced methods to measure the CEO frequency. We have also analyzed sources of CEO-phase noise and given guidelines on how to increase the passive stability of the CEO phase. Even if such measures can be further improved, the residual noise of the free-running laser is still prohibitive for many applications in extreme nonlinear optics, which demand a stable CEO phase for seconds or minutes of integration times.

## 5.1 Controlling the CEO frequency of a laser oscillator

The only missing link to stabilization of the CEO frequency is now a mechanism for external control of the CEO frequency. Such a mechanism allows closing the servo loop, forcing the CEO frequency into a lock with an rf-reference oscillator. Ideally, a control mechanism should only act on the CEO frequency and leave other cavity parameters unchanged (orthogonality). If we leave this concern aside, all mechanisms causing APC are suited, in principle, for control of the CEO frequency. As was discussed previously, a servo bandwidth of more than 10 kHz is needed, which rules



out many slow mechanisms. Choice of the control mechanism is therefore a trade-off between orthogonality and bandwidth.

In lasers with intracavity prism sequences, an elegant way of controlling the CEO frequency of a laser without affecting other laser parameters is offered. Tilting the end mirror after the prism sequence affects only the difference between the group and phase delay in the cavity but leaves other laser parameters widely unchanged [12, 29]. The tilt of the end mirror has to be restricted to small excursions compared to the angular aperture of the beam at the end mirror. Only then can one be sure that the intracavity power is not also affected by the mirror tilt. Mirror excursion in the microradian range is sufficient to control the CEO frequency within one spectral range. This makes mirror tilting the method of choice for cavities with prisms. However, it is typically very difficult to reach a servo bandwidth of more than 1 kHz with mirror tilting because of mirror inertia. Reaching sufficient bandwidth requires an optimized setup of the tilt actuator. Bandwidths up to 25 kHz have been demonstrated using a mirror of low mass directly mounted on a split piezoelectric transducer (PZT) actuator [30].

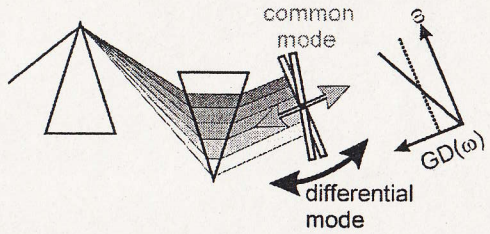


*Figure 5-10.* Control of intracavity first-order dispersion by tilting of an end mirror after a dispersive delay line. Translation of the mirror parallel to the optical axis acts on both group and phase delay; tilting changes the difference between them. Provided a choice of the correct pivot point has been made, tilting only affects the CEO-frequency.

Mirror tilting is not an option when a prismless setup is used. Then the method of choice is modulation of the pump power either with an acousto-optic modulator [16] or with an electro-optic device [20]. As the required pump-power modulation is on the order of $10^{-3}$, it is typically very easy to reach bandwidths of several tens to hundreds of kHz. Pump-power modulation relies on the APC mechanisms discussed in the previous section and is currently the most widespread mechanism for CEO-frequency control.

## 5.2 Performance of CEO phase locks

Several detailed investigations on stabilization of the CEO frequency and the resultant residual CEO phase noise have been published [16, 20, 21, 30]. All these authors used microstructure fibers for additional external

broadening of the laser spectra. A first attempt to directly stabilize the CEO frequency of an octave-spanning laser was reported by Morgner et al. [3]. However, because this laser only spanned the octave at about -40 dBc, the authors achieved a CEO beat note that was considered minimum for a robust stabilization. The authors thus proposed a $2\nu$-to-$3\nu$ scheme. This scheme has been carried out recently with resulting small residual timing jitters and excellent long-term stability [31]. Still, a direct stabilization is more challenging than stabilization based on additional spectral broadening.

Another important issue is the setup of the locking electronics. For any meaningful application, a phase lock to an rf-reference source is required. A phase lock can be as simple as that depicted in Figure 5-11, which consists of a double-balanced mixer and some means to adjust the servo loop gain. The gain has to be optimized for a sufficient phase margin of the loop to prevent self-oscillation of the servo circuit.

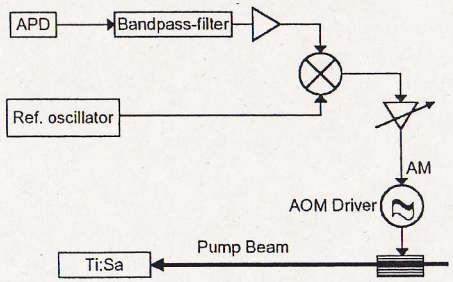


*Figure 5-11.* Simple phase-lock circuit used for stabilization of the CEO frequency [16]. The avalanche photo detector (APD) measures the beat note signal [Equation (6), Figure 5-5]. Suitable bandpass filtering isolates the beat note and suppresses mirror frequencies and spurious contributions. After mixing the signal with the reference oscillator, the mixing product is directly fed back via an acousto-optic modulator. The servo loop gain has to be adjusted for sufficient phase margin.

The simple circuit of Figure 5-11 has only a very limited capture range and may not be able to avoid cycle slips in the presence of strong CEO-phase noise. An alternative is usage of a phase detector with enhanced capture range [32]. Such a circuit is based on an electronic counter and can boost the phase capture range to tens or hundreds of $\pi$. This strategy comes at the price of decreased sensitivity that will ultimately limit the overall performance of the lock. The general recommendation is to reduce noise mechanisms as far as possible by enhancing the passive stability of the laser. Capture range enhancement should only be used as a last resort and then moderately; otherwise, extra noise of the stabilized laser will result.



Some of the best results in terms of residual phase noise were achieved with the simple double-balanced mixer (Reference [16], Figure 5-11). The measured data is also shown in Figures 5-7 and 5-8. From the data in Figure 5-8, one can conclude that the residual phase jitter in these measurements was only about 20 mrad in a 10 kHz to 0.01 Hz interval. This corresponds to residual timing jitters of only 10 as associated with the CEO phase.

## 5.3 Limitations of CEO control

Using additional external broadening in a piece of microstructure fiber is currently the most widespread method for measuring and stabilizing the CEO frequency. As APC effects play a strong role in intracavity CEO dynamics, it would be surprising if the strong Kerr nonlinearities involved in continuum generation would not also give rise to APC effects extracavity. There is an important difference that immediately explains why extracavity APC effects are a much lesser concern than the effects discussed in Section 4.4. If the same element with identical amplitude-to-phase coupling is moved from intracavity to extracavity, it generates CEO-phase noise via

$$\sigma_{\phi_{ce}}^{(extracavity)}(f) = \frac{1}{f_r}\sigma_{f_0}^{(intracavity)}(f). \qquad (11)$$

The highest measured noise densities of the prismless oscillator of $\sigma_{f_0}^{(intracavity)} \approx 1\,\mathrm{kHz}/\sqrt{\mathrm{Hz}}$ would therefore translate into extracavity-phase noise densities of only $\sigma_{\phi_{ce}}^{(extracavity)} \approx 10^{-5}\,\mathrm{rad}/\sqrt{\mathrm{Hz}}$.

Several approaches to experimentally quantify the strength of extracavity APC have been reported. Fortier et al. measured a coupling coefficient of 3.8 rad/pJ for a 100 MHz laser [33]. These measurements relied on an out-of-loop characterization of the stabilized oscillator, employing a second totally independent microstructure fiber and a second $\nu$-to-$2\nu$ interferometer. A differential CEO-phase measurement using two independent CEO-measurement schemes was reported in [8]. In this measurement, two independent CEO measurements on the same source were compared. A differential phase-noise spectrum is displayed in Figure 5-12. One can immediately see that the residual uncertainty of the CEO-phase measurement is several orders of magnitude smaller than the phase noise of the free-running oscillator. The phase noise shown in Figure 5-12 adds up to an rms value of about $\pi$ in a 5 s integration time [compare Equation (9) and Figure 5-8]. The differential phase noise is mainly due to slow drifts that can corrupt measurements at long integration times.

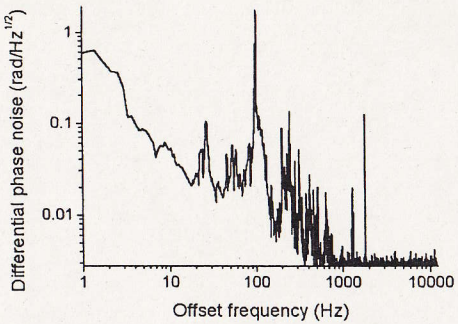


*Figure 5-12.* Differential phase-noise spectrum of two independent measurements of the CEO phase.

Several ways have been suggested for overcoming these residual effects. Rather than using the laser pulses directly, one can use the white-light continuum pulses for any kind of CEO-sensitive application. Using the spectrum directly from an octave-spanning oscillator would also rule out APC effects in the microstructure fiber. Still, both these solutions suffer from interferometer drift. One way to strongly reduce drift effects is a common-path interferometer, as suggested by Kakehata et al. [34] for single-shot CEO-phase measurements.

## 6. SUMMARY

We have discussed fluctuations of the CEO phase in oscillators and explained their origin. The CEO phase turns out to be a very sensitive parameter that is easily influenced by nearly all laser and environmental parameters. Many of these contributions either give rise to slow drift effects or can be easily shielded by enclosing the laser. From the perspective of stabilizing the CEO frequency of the laser, however, amplitude-to-phase noise conversion turns out to be a much more significant problem that cannot totally be avoided. Several mechanisms contribute to the conversion of laser amplitude noise into CEO frequency fluctuations. Again, some of these contributions, such as spectral shifting or beam pointing, can be avoided, or at least reduced, by construction and choice of favorable operating conditions. With all these measures in place, it is possible to provide a tight lock to an external rf reference, with resulting residual timing jitters between carrier and envelope of the laser of only a few attoseconds. Even with such superior performance, one has to be careful to avoid intrinsic sources of CEO phase noise in the measurement set-up itself. Amplitude-to-phase conversion also takes place in external continuum generation, which is often used to broaden the laser spectrum to an optical octave. The $\nu$-to-$2\nu$ interferometer is another weak point and can give rise to a small residual drift. These residual effects are relatively weak and do not appear to corrupt most applications of frequency combs demonstrated to date. Nevertheless, they can be avoided. An improved control of frequency comb parameters offers even higher precision in metrology applications and opens up novel applications in extreme nonlinear optics. Understanding the dynamics of the comb is the key to further progress in these areas.



## REFERENCES

[1] G. Steinmeyer, D. H. Sutter, L. Gallmann, N. Matuschek, and U. Keller, Science **286**, 1507-1512 (1999); U. Keller, Nature **424**, 831-838 (2003).

[2] M. Nisoli, S. Desilvestri, O. Svelto, R. Szipocs, K. Ferencz, C. Spielmann, S. Sartania, and F. Krausz, Opt. Lett. **22**, 522-524 (1997); A. Baltuška, M. S. Pshenichnikov, and D. A. Wiersma, Opt. Lett. **23**, 1474-1476 (1998); A. Baltuška, T. Fuji, and T. Kobayashi, Opt. Lett. **27**, 1241-1243 (2002); R. Ell, U. Morgner, F. X. Kärtner, J. G. Fujimoto, E. P. Ippen, V. Scheuer, G. Angelow, T. Tschudi, M. J. Lederer, A. Boiko, and B. Luther-Davies, Opt. Lett. **26**, 373-375 (2001).

[3] U. Morgner, R. Ell, G. Metzler, T. R. Schibli, F. X. Kärtner, J. G. Fujimoto, H. A. Haus, and E. P. Ippen, Phys. Rev. Lett. **86**, 5462-5465 (2001).

[4] D. H. Sutter, G. Steinmeyer, L. Gallmann, N. Matuschek, F. Morier-Genoud, U. Keller, V. Scheuer, G. Angelow, and T. Tschudi, Opt. Lett. **24**, 631-633 (1999).

[5] G. G. Paulus, F. Grasbon, H. Walther, P. Villoresi, M. Nisoli, S. Stagira, E. Priori, and S. De Silvestri, Nature **414**, 182-184 (2001); G. G. Paulus, F. Lindner, H. Walther, A. Baltuška, E. Goulielmakis, M. Lezius, and F. Krausz, Phys. Rev. Lett. **91**, 253004 (2003).

[6] H. R. Telle, G. Steinmeyer, A. E. Dunlop, J. Stenger, D. H. Sutter, and U. Keller, Appl. Phys. B **69**, 327-332 (1999).

[7] T. Brabec and F. Krausz, Rev. Mod. Phys. **72**, 545-591 (2000).

[8] F. W. Helbing, G. Steinmeyer, and U. Keller, IEEE J. Sel. Top. Quantum Electron. **9**, 1030-1040 (2003).

[9] T. Udem, J. Reichert, R. Holzwarth, and T. W. Hänsch, Opt. Lett. **24**, 881-883 (1999).

[10] T. F. Albrecht, K. Bott, T. Meier, A. Schulze, M. Koch, S. T. Cundiff, J. Feldmann, W. Stolz, P. Thomas, S. W. Koch, and E. O. Göbel, Phys. Rev. B **54**, 4436-4439 (1996).

[11] N. Haverkamp, B. Lipphardt, J. Stenger, H. R. Telle, C. Fallnich, and H. Hundertmark, In *Conference On Ultrafast Phenomena*, Vancouver, BC, 2002), P. Me31-31.

[12] K. F. Kwong, D. Yankelevich, K. C. Chu, J. P. Heritage, and A. Dienes, Opt. Lett. **18**, 558-560 (1993).

[13] L. Xu, C. Spielmann, A. Poppe, T. Brabec, F. Krausz, and T. W. Hänsch, Opt. Lett. **21**, 2008-2010 (1996).

[14] D. J. Jones, S. A. Diddams, J. K. Ranka, A. Stentz, R. S. Windeler, J. L. Hall, and S. T. Cundiff, Science **288**, 635-639 (2000).

[15] A. Apolonski, A. Poppe, G. Tempea, C. Spielmann, T. Udem, R. Holzwarth, T. W. Hänsch, and F. Krausz, Phys. Rev. Lett. **85**, 740-743 (2000).
[16] F. W. Helbing, G. Steinmeyer, U. Keller, R. S. Windeler, J. Stenger, and H. R. Telle, Opt. Lett. **27**, 194-196 (2002).
[17] H. R. Telle, D. Meschede, and T. W. Hänsch, Opt. Lett. **15**, 532-534 (1990).
[18] U. Keller, K. D. Li, M. Rodwell, and D. M. Bloom, IEEE J. Quantum Electron. **25**, 280-288 (1989).
[19] R. P. Scott, C. Langrock, and B. H. Kolner, IEEE J. Sel. Top. Quantum Electron. **7**, 641-655 (2001).
[20] A. Poppe, R. Holzwarth, A. Apolonski, G. Tempea, C. Spielmann, T. W. Hansch, and F. Krausz, Appl. Phys. B **72**, 373-376 (2001).
[21] F. W. Helbing, G. Steinmeyer, J. Stenger, H. R. Telle, and U. Keller, Appl. Phys. B **74**, S35-S42 (2002).
[22] H. R. Telle, In *Frequency Control Of Semiconductor Lasers*, Edited By M. Ohtsu (John Wiley & Sons, New York, 1996), P. 137-167.
[23] K. W. Holman, R. J. Jones, A. Marian, S. T. Cundiff, and J. Ye, Opt. Lett. **28**, 851-853 (2003).
[24] R. L. Fork, O. E. Martinez, and J. P. Gordon, Opt. Lett. 9, 150-152 (1984); R. E. Sherriff, J. Opt. Soc. Am. B **15**, 1224-1230 (1998).
[25] J. Stenger and H. R. Telle, Opt. Lett. **25**, 1553-1555 (2000); H. A. Haus and E. P. Ippen, Opt. Lett. **26**, 1654-1656 (2001).
[26] G. P. Agrawal, *Nonlinear Optics* (Academic Press, San Diego, 2001).
[27] M. Sheikbahae, D. C. Hutchings, D. J. Hagan, and E. W. Van Stryland, IEEE J. Quantum Electron. **27**, 1296-1309 (1991).
[28] R. Desalvo, A. A. Said, D. J. Hagan, E. W. Van Stryland, and M. Sheik-Bahae, IEEE J. Quantum Electron. **32**, 1324-1333 (1996).
[29] J. Reichert, R. Holzwarth, T. Udem, and T. W. Hänsch, Opt. Commun. **172**, 59-68 (1999).
[30] T. M. Fortier, D. J. Jones, J. Ye, S. T. Cundiff, and R. S. Windeler, Opt. Lett. **27**, 1436-1438 (2002).
[31] A. Bartels, S. A. Diddams, T. M. Ramond, and L. Hollberg, Opt. Lett. **28**, 663-665 (2003).
[32] U. Tietze, C. Schenk, and E. Schmid, *Electronic Circuits: Design And Applications* (Springer, New York, 1991).
[33] T. M. Fortier, J. Ye, S. T. Cundiff, and R. S. Windeler, Opt. Lett. **27**, 445-447 (2002).
[34] M. Kakehata, Y. Fujihira, H. Takada, Y. Kobayashi, K. Torizuka, T. Homma, and H. Takahashi, Appl. Phys. B **74**, S43-S50 (2002).

# Chapter 6

# FEMTOSECOND NONCOLLINEAR PARAMETRIC AMPLIFICATION AND CARRIER-ENVELOPE PHASE CONTROL

Takayoshi Kobayashi
*Department of Physics, Faculty of Science, University of Tokyo*

**Abstract:** This chapter presents the basic principles for three parametric interactions that enhance bandwidth to obtain short pulses while maintaining phase matching. To extend the bandwidth, we introduced a noncollinear configuration between the pump and signal. The idea is used in three different parametric processes: optical parametric generation (OPG), optical parametric amplification (OPA), and optical parametric oscillation (OPO). Using noncollinear phase matching, we developed a noncollinear-optical-parametric amplifier (NOPA) that delivers 4 fs visible-near-infrared pulses. We designed geometrical and temporal configurations of the NOPA that broaden the gain bandwidth in excess of 250 THz. The main requirements for bandwidth enhancement include (1) phase matching, (2) group-velocity matching, (3) pulse-front matching, and (4) optimization of the angular dispersion of the pump. To achieve the extended-gain bandwidth, full phase adjustment is performed by several compensators, including a prism pair, a grating-mirror system equivalent to a grating pair, chirped mirrors, and a deformable mirror. By adding these devices to the NOPA system, we obtained pulse widths of 3.9 fs in the visible and NIR spectral range.

**Key words:** carrier-envelope phase, optical parametric amplification

## 1. INTRODUCTION

Femtosecond laser systems are experiencing explosive growth in both the number of users and variety of applications. In the process, pulse duration is continually being reduced. Optical pulses with a duration of only a few optical cycles have been achieved with the proliferation of diverse types of Ti:sapphire lasers. Sub-5 fs pulses have become available with 800 nm